Hindawi
Journal of Nanomaterials
Volume 2022, Article ID 7712859, 11 pages
https://doi.org/10.1155/2022/7712859

Research Article

Application of New Energy Composites in Sports Facilities and Fitness Equipment

Jiejian Zhang[1,2] and Yang Mi[3,4]

[1]*Department of Physical Education, Science and Technology College Gannan Normal University, Ganzhou, 341000 Jiangxi, China*
[2]*Department of Leisure Sports, Jungwon University, Chungbuk 28024, Republic of Korea*
[3]*School of Sports and Health, Linyi University, Linyi, 276000 Shandong, China*
[4]*Department of Physical Education, Woosuk University, Jeonju 55069, Republic of Korea*

Correspondence should be addressed to Yang Mi; miyang@lyu.edu.cn

Received 28 February 2022; Revised 30 March 2022; Accepted 15 April 2022; Published 28 April 2022

Academic Editor: Awais Ahmed

New energy composite is an advanced material that can replace the traditional single metal material, especially the newly developed or developed material with superior performance. At present, the material is widely used in automobile manufacturing and other fields, but there is a lack of development and application of the material in the field of sports. To solve these problems, this paper puts forward the application of new energy composites in sports facilities and fitness equipment. In this paper, the testing methods of new energy materials, including thermoelectric testing method and energy absorption testing method, can quantitatively evaluate the properties of a kind of new energy composites and point out the direction for the development of materials with high thermoelectric properties and high-energy absorption and consumption properties. Then, through the preparation experiment of new energy materials, this paper studies the preparation process and self-shrinkage test of carbon nanomaterials. Finally, it is proposed to use carbon nanomaterials in the sensor design of health monitoring data acquisition system. The experimental results show that when the water ash ratio is low, the self-shrinkage value of carbon nanomaterial slurry is 74.68% lower than that under the original conditions. In the experimental study of omnidirectional monitoring characteristics, through the repeated tensile tests of rectangular sensor and omnidirectional sensor at different temperatures, it is found that the sensitivity coefficient of the sensor made of carbon nanomaterial is between 55.8 and 60.4, and the maximum fluctuation is only 5. This fully proves that the carbon nanotube omnidirectional sensor has omnidirectional detection ability.

1. Introduction

1.1. Background. Since the birth of human civilization, material has been closely related to human life. There are generally three forms of matter in nature, namely, solid, liquid, and gas. With the development and progress of science and technology, materials not only penetrate into people's daily life, but also are widely used in aerospace, marine engineering, biomedical engineering, optoelectronics, and other fields. This article observes that new energy materials may also be applicable to the field of sports. New materials refer to some newly developed or under research and development materials with excellent performance, mainly including superconducting materials, solar cell materials, hydrogen storage materials, solid oxide cell materials, intelligent materials, magnetic materials, nanomaterials, high-temperature structural ceramics, amorphous materials, and high-density energy storage materials. Composite material refers to the new material composed of material components of different properties by using advanced material preparation technology.

1.2. Significance. Under the background of global fossil energy shortages and environmental pollution, the development of high-performance thermoelectric materials and efficient new energy technologies has attracted extensive attention in the industry. The composite material not only maintains the advantages of the material properties of each component, but also obtains the comprehensive performance that cannot be achieved by a single component material through the complementarity and correlation of the properties of each component. Human beings also need to systematically study the durability of carbon nanomaterials and other cement-based composites. The unique one-dimensional structure of carbon nanotubes and nanofibers and the two-dimensional structure of graphene, as well as the advantages of compact structure, large specific surface area, and high strength of carbon nanomaterials, can effectively transport water in cement through the landfill matrix and holes in the matrix, improve the compactness of cement materials, and further improve the durability such as impermeability and corrosion resistance. On the basis of improving the self-shrinkage properties of carbon nanomaterial and cement-based composites, other durability properties of carbon nanomaterial and cement-based composites can be systematically studied to improve their safety and service life, which is of great engineering significance and value. With the popularization of high-performance concrete with low ratio of water and binder, the crack phenomenon caused by early automatic shrinkage of concrete is becoming increasingly obvious. Adding carbon nanomaterials into cement materials can not only effectively fill the pores of the cement matrix, but also increase the content of hydration products, to improve the density of matrix.

1.3. Related Work. The role of new energy and composite material, materials, and sports equipment in human life is becoming increasingly obvious, and many scholars have carried out research on these two topics. Wang Q believes that, under the background of establishing emerging engineering education, the content of organic chemistry of material engineering needs innovation. He strives to improve the application effect of organic chemistry from the aspects of material preparation and material application, selection, process, method reform, improvement of evaluation system, and optimization of organic chemistry experiments. His research focuses on the application expansion of materials, but ignores the detailed manufacturing innovation of materials [1]. Martinho F pointed out that the monolithic series integration of third-generation solar materials on silicon has broad prospects in the fields of photoelectrochemistry and photovoltaics. However, this may be challenging when involving the high-temperature reaction process, which may damage the bottom cell of photovoltaic equipment. They have proved that the protection of the bottom cell of photovoltaic equipment largely depends on the barrier layer engineering at the device level, but their research has not produced several single-chip series solar cells, which is limited to the application of new energy materials [2]. Mansurov Z A studied the effect of activated carbon with multilayer graphene (three layers and more sheets) on the thermal decomposition of substances based on hydroxyammonium nitrate and carboxymethyl cellulose. His results showed that the addition of activated carbon with multilayer graphene could increase the combustion rate of hydroxyammonium nitrate by up to four times; however, in the experiment, the addition of activated carbon in the thermal decomposition stage reduced the temperature and time of chemical reaction, resulting in some deviations in the experimental results [3]. Paben J believes that the flexible packaging material will not disappear soon, and the upcoming pilot project aims to ensure that it will not enter the landfill. He proposed a material recycling facility, which will install additional sorting equipment. The transformation will enable the facility to start producing postconsumer flexible packaging bags, which are defined as single-layer or multilayer material films, expanding the source mode of new energy materials. However, he did not explain the defects of materials made from recycled raw materials [4]. Tao Kunwei studied the compact materials project, which will provide a high-energy, high-throughput neutron source for material irradiation research, which is essential for advanced nuclear energy projects driven by China's long-term accelerators. He introduced a numerical study of a particle beryllium targets using inclined particle flow as the target and heat carrier. To study the heat treatment capacity of the target as a sports facility, the heat deposition and transfer in the target were numerically simulated. However, his research damaged the back plate of the experimental material in terms of heat dissipation and radiation [5]. Lee J Y evaluated the function of a dual water supply system operating in sports facilities based on technical, quantitative, and financial data, including the collection and use of rainwater for nonpotable purposes. Analysis was conducted to determine the water-saving efficiency and cost reduction of the facility within 3 years. The results show that rainwater can be managed for the benefit of the environment, and economic benefits can be obtained by saving the water cost of municipal water supply and sewage treatment. However, the results of this study are not encouraged because of the overexploitation of groundwater [6]. Sukiri's research aims to determine customer satisfaction with the services and fitness equipment of the academic gymnasium of the School of Sports Science, Jakarta State University. He made a questionnaire and published it using Google forms. His research used survey and descriptive analysis. According to the data returned by the interviewees, the average interviewee was satisfied with the facility, but did not pay attention to the interviewee's satisfaction with the facility [7]. Thakur T S believes that cycling and other sports activities are a healthy, interesting, and low impact way of exercise, which is suitable for people of all ages. His research paper covers the evolution of sports facilities from ancient times to modern times. Through this study, he has tried to study the transformation of sports facilities through a wide range of technical applications to improve and enhance their functions, but his research focuses on the improvement of bicycles and does not extend the research results to other fitness equipment [8]. The deficiency of these studies is that the research methods and perspectives are still not novel and comprehensive enough.

1.4. Innovation Points. This paper boldly puts forward the application of new energy materials in the field of sports and expands the application scope of new energy materials. The most representative carbon nanomaterials in new energy materials are used to prepare motion monitoring sensors, which expands the new idea of sensor design.

2. Performance Test Methods of New Energy Materials

2.1. Thermoelectric Test Method for New Energy Composites. New energy composites are made by combining two or more fibers in a matrix. New energy composites have the characteristics of high strength, elastic modulus, and excellent mechanical properties. Mechanical characteristics are also relatively good, which can fully meet the requirements and make them a popular choice for light weight and high-performance applications. Because the cost of carbon fiber is too high, the combination of glass fiber and carbon fiber is needed to obtain reliable mechanical properties [9]. The new energy composites with mixed carbon fiber and glass fiber have a good balance in mechanical properties; that is, the disadvantages of one fiber can be offset by the advantages of another fiber [10]. In addition to the mixed structure, the strength, damage resistance, and service life of new energy composites can be improved by changing the microstructure of materials. However, the mixing and aggregation of fibers have a significant impact on the elastic properties of the composites. On the one hand, it is the microstructure characteristics of fibers, namely, the aggregation of fibers and the distribution of fibers in the aggregation area, a small amount of bonding between the foundation and fibers, bending effect, and unevenly distributed fibers, that will weaken the mechanical properties of composites [11]. On the other hand, it is generally believed that the experimental mechanical properties of new energy composites are far from the theoretical prediction results. Therefore, it is of great significance to determine the influence of these defects on the effective properties of new energy composites.

The content of the experimental method is the thermoelectric test of materials. Firstly, the key technical indexes of thermoelectric performance test are analyzed. All relevant metrics were analyzed in detail. According to the thermoelectric performance test principle, the signal acquisition circuit required for corresponding parameter measurement is designed, and the thermoelectric performance test platform is built to realize the automatic measurement of thermoelectric performance parameters of new energy materials [12].

Seebeck coefficient is the ratio of voltage to temperature difference generated by Seebeck effect, which represents the ionization impurity scattering coefficient [13]. Assuming that only the electric field and temperature gradient of the material are in a stable state, and the material is a nondegenerate semiconductor, the relaxation time is approximately obtained according to the Boltzmann equation. Then, the Seebeck coefficient of the material is shown in

$$\mathrm{A} = \pm \frac{\mathrm{k_B}}{\mathrm{e}}\left[\mathrm{b} - \left(\mathrm{s} + \frac{5}{2}\right)\right], \tag{1}$$

where s is the scattering coefficient and B is the reduced Fermi level. Therefore, if semiconductor thermoelectric materials are doped, the ionized impurity concentration increases, and the ionized impurity scattering coefficient increases [14]. If the large ionized impurities are scattered (high concentration of ionization impurities), the Seebeck coefficient corresponding to the specified carrier concentration is greatly improved, and the thermoelectric performance is improved. If the material is a single band nondegenerate semiconductor, the Seebeck coefficient of the material can be expressed by

$$A = \pm \frac{k_B}{e}\left[b - \left(s + \ln \frac{N}{n}\right)\right] \tag{2}$$

Therefore, the Seebeck coefficient of materials is related to carrier concentration, state density, Fermi energy level, scattering coefficient, and other physical quantities. In formula (2), n is the state density, and N is the carrier concentration.

When calculating the conductivity of materials, the expression of conductivity q is Q = neu. In the formula, n is the carrier concentration, and u is the error rate.

$$n = \frac{2(2\pi m^* k_B T)^{1.5}}{h^{1.5}} F_{s+0.5}(b), u = \frac{4e}{3\pi^{1/2}}(s + 1.5)(k_B T)^s \frac{t_0}{m^*}, \tag{3}$$

where $m*$ is the effective mass of the carrier, h is the Planck constant, and t0 is the relaxation time. Formula (3) shows that the conductivity is affected by the scattering coefficient, effective mass, Fermi level, and other factors, and the carrier concentration and mobility do not necessarily increase at the same time. When the effective mass of the material increases, the carrier concentration increases, and the mobility decreases [15]. If the mobility decreases, the conductivity and thermal conductivity decrease at the same time.

From the microscopic point of view, the transmission process of heat energy is mainly realized by carrier motion and lattice vibration. In the case of semiconductor materials in the intrinsic state and semiconductor materials in the exogenous excitation region, only the contribution of carrier and lattice phonons to the thermal conductivity must be considered [16]. In other words, $k = k_{ph} + k_c$, where k_{ph} is the phonon thermal conductivity and k_c is the thermal conductivity of the carrier. General thermoelectric materials are applicable in the exogenous excitation stage. Therefore, only the contribution of carrier thermal conductivity and phonon thermal conductivity to thermal conductivity must be considered [17]. At the beginning of the twentieth century, Altengilsch of Germany put forward the analysis of three important parameters affecting thermoelectric properties and put forward the thermoelectric performance index Z to measure the thermoelectric properties of materials.

$$Z = \frac{A^2 Q}{k}, E = A^2 Q, \tag{4}$$

where a is the Seebeck coefficient, K is the thermal conductivity, q is the conductivity, and E is the power factor. This formula can be used to reflect the comprehensive thermoelectric properties of materials. The larger the Z value, the higher the thermoelectric properties of the material. Therefore, for materials with good thermoelectric characteristics, the Seebeck coefficient is large; that is, the obvious thermoelectric effect requires the conductivity Q to be as large as possible, and the thermal conductivity must be K small with less Joule heat. Materials with high thermoelectric properties point out the direction for the production of new energy composites [18].

2.2. Test Method for Energy Absorption of Materials. Sports facilities and fitness equipment have high mechanical requirements for materials, and the manufacturing materials must have strong energy absorption capacity in order to meet the sports facilities and fitness equipment for the material strength requirements. This paper has mentioned that the new energy material absorber achieves impedance matching conditions by adjusting the electromagnetic parameters, to reduce reflection and achieve high absorption, because the reflection is actually caused by the impedance mismatch with the material surface. However, the use of impedance matching theory means that new energy materials need to be regarded as a whole; that is, their optical properties can be described by macroscopic optical parameters impedance Z and refractive index n [19]. According to the equivalent media theory (theory of composite properties), the structural unit of new energy materials is a subwavelength size smaller than its working wavelength, so they can be regarded as a whole. Moreover, their electromagnetic characteristics can be expressed by the equivalent permeability Ueff and equivalent dielectric constant Eeff [20].

In free space, the impedance Z, refractive index n, dielectric constant e, permeability u, and reflectivity R are assumed. If a uniform plate with thickness D, when the electromagnetic wave with angular frequency w is vertically incident on one side of the material plate, its transmission performance can be expressed by the reflection coefficient F and transmission coefficient T [21]. The expression is as follows:

$$\frac{f}{t} = -\frac{i}{2}\left(Z - \frac{1}{Z}\right) \sin \text{nkd}, \tag{5}$$

$$t^{-1} = \left[\sin\left(\text{nkd}\right) - \frac{i}{2}\left(Z - \frac{1}{Z}\right) \cos\left(\text{nkd}\right)\right] e^{\text{ikd}}. \tag{6}$$

The principle of magnetic wave vertical incidence is shown in Figure 1.

Under the condition of impedance matching, it can be seen that the reflection coefficient r tends to 0, while the transmission coefficient T can be reduced to the exponential form:

$$t^{-1} = e^{-i(n_1-1)kd} * e^{n_2 kd}. \tag{7}$$

At this time, there are two limit cases for the transmittance of the material $t = |t|2$. In the first case, when the transmittance T and reflectivity R are both 0, the absorbance A is 1, and the electromagnetic wave is completely absorbed. The second case is that the reflectivity R and absorptivity a are 0 and the transmittance t is 1. At this time, the material neither reflects nor absorbs electromagnetic waves, realizing perfect stealth [22]. For energy absorption by new energy materials, only the first case is considered in this paper. At this time, there are

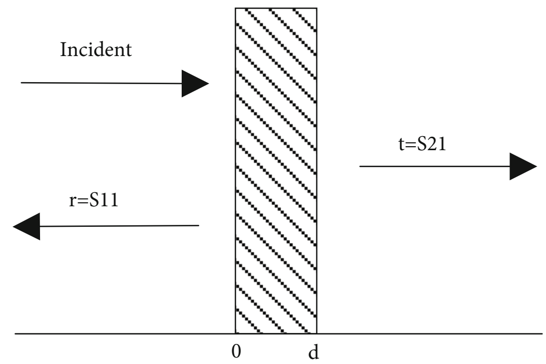

Figure 1: Schematic diagram of scattering parameters of electromagnetic new energy materials.

$$\lim_{n2\longrightarrow\infty} T = |t|^2 = \lim_{n2\longrightarrow\infty} e^{-2n_2 kd} = 0. \tag{8}$$

Since t only tends to 0 in the actual structure, $N2$ usually shows a large peak. It can be seen that the design of new energy materials to absorb energy is actually to design a structure with appropriate dielectric constant Eeff and permeability Ueff to meet the impedance matching conditions, reduce the reflectivity r to 0, reduce the transmittance t as much as possible, and consume the energy of electromagnetic wave inside the structure as much as possible, to obtain high absorption [23].

3. Preparation, Experiment, and Application of New Energy Materials

3.1. Preparation of Carbon Nanomaterials. In this paper, the representative carbon nanomaterials in new energy materials are selected to study their preparation and application process. The preparation and application of carbon nanomaterials are beneficial to improve the material quality of exercise equipment. In this paper, the effects of different carbon nanomaterial content, water-cement ratio, and test age on the self-shrinkage properties of cement paste samples were studied: (1) three water-cement ratios of 0.25, 0.30, and 0.35 were selected to study the changes of self-shrinkage properties of carbon nanomaterial cement paste with water-cement ratio. (2) Six contents of 0.05 wt%, 0.075 wt%, 0.1 wt%, 0.12 wt%, and 0.15 wt% were selected to study the effects of different carbon nanomaterial contents on the self-shrinkage properties of cement paste composites. Choosing different doses of nanomaterials for research allows for a full understanding of carbon nanomaterials properties. (3) The self-shrinkage values of three kinds of carbon nanomaterial and cement-based composites were measured every 1 min by self-shrinkage tester to study the self-shrinkage characteristics of carbon nanomaterial and cement paste composites. To ensure the good workability of the specimens with low water-cement ratio, a certain amount of polycarboxylic acid water reducer was added in the preparation process.

The dispersant of multilayer carbon nanotubes is gum Arabic, and the mass ratio of multilayer carbon nanotubes to gum Arabic is 1 : 6. In addition, a certain amount of defoamer needs to be added to the prepared multiwall carbon nanotube suspension [24]. Through experimental exploration, it is determined that the addition of 0.13 wt% tributyl phosphate defoamer can eliminate the bubbles generated in the ultrasonic process of multiwall carbon nanotube suspension. The mix proportion design of high-performance multiwall carbon nanotube cement-based composites is shown in Table 1.

The dispersant of carbon nanofibers is methylcellulose, and the two mass ratios are 1 : 2. Moreover, a certain amount of defoamer must be added to the prepared carbon nanofiber suspension. The experimental investigation results show that if 0.15 wt% tributyl phosphate defoamer is added, the bubbles generated by the carbon nanofiber suspension can be removed in the ultrasonic process [25].Table 2 shows the ratio of basic composites to high-performance carbon nanofiber products.

The dispersant of graphene (GNP) is polyethylene vinyl phenyl ether (co 890), and the mass ratio of GNP to co 890 is 1 : 5. In addition, a certain amount of defoamer must be added to the prepared graphene suspension. The experimental investigation shows that the addition of 0.20 wt% three-phosphate butyl defoamers can eliminate the foam [26] formed by the suspension of graphene in an ultrasonic process.

3.2. Self-Shrinkage Test Results of Carbon Nanomaterials. The effects of multiwalled carbon nanotube content, water-cement ratio, age, and surfactant Arabic gum on the self-shrinkage of cement paste that were studied here are some results from the above tests.

(1) Under the same water-cement ratio, the self-shrinkage of multiwalled carbon nanotube cement paste changes with age.

Under the condition of the same water-cement ratio, the change of self-shrinkage performance of multiwall carbon nanotube cement paste with age is shown in Figure 2.

It can be seen from these four figures that when the water-cement ratio is 0.30 and 0.35, the automatic shrinkage value of multilayer carbon nanotube cement paste test piece first decreases and then increases with the increase of age. When the water-cement ratio is 0.25, the autogenous shrinkage value of the specimen increases with age, especially from the initial setting time to the first day of the test time. When the test age increases to 7 days (w/C = 0.35 and 0.30) or 14 days (w/C = 0.25), the growth rate of self-shrinkage value of MWCNT cement paste is very small, the growth rate of self-shrinkage value is slow, and the self-shrinkage curve tends to be stable. Because the reaction between cement and water is heating, the temperature of the sample increases, resulting in thermal expansion. The early heating reaction of cement is intense, and the hydration reaction will release a lot of heat, causing the thermal expansion of the cement, to offset part of the self-shrinkage. The self-shrinkage value at this time is actually the combined result of thermal expansion and self-shrinkage. When the water-cement ratio is 0.3 and 0.35, respectively, on the first day of measurement, the expansion value caused by thermal expansion is greater than the self-shrinkage value, resulting in the decline of the self-shrinkage curve, and the self-shrinkage value is negative [27]. Then, with the increase of age, the hydration reaction of cement slows down gradually, which weakens the thermal expansion phenomenon, and the self-shrinkage value is gradually greater than the expansion value, which makes the self-shrinkage curve rise and the

Table 1: Mix proportion of high-performance multiwall carbon nanotube cement-based composites.

Sample serial number	Water-cement ratio W/C	MWCNTs/ wt%	GA/ wt%	TBP/ wt%	PS/ wt%
S25-A-0	0.25	0.00	0.00	0.13	0.60
S25-A-1	0.25	0.05	0.30	0.13	0.60
S25-A-2	0.25	0.07	0.45	0.13	0.60
S25-A-3	0.25	0.10	0.60	0.13	0.60
S25-A-4	0.25	0.12	0.72	0.13	0.60
S30-A-0	0.30	0.00	0.00	0.13	0.20
S30-A-1	0.30	0.05	0.30	0.13	0.20
S30-A-2	0.30	0.07	0.45	0.13	0.20
S30-A-3	0.30	0.10	0.60	0.13	0.20
S30-A-4	0.30	0.12	0.72	0.13	0.20
S35-A-0	0.35	0.00	0.00	0.13	0.00
S35-A-1	0.35	0.05	0.30	0.13	0.00
S35-A-2	0.35	0.07	0.45	0.13	0.00
S35-A-3	0.35	0.10	0.60	0.13	0.00
S35-A-4	0.35	0.12	0.72	0.13	0.00

Table 2: Mixing ratio of high-performance nanocarbon fiber cement-based composites.

Sample serial number	Water-cement ratio W/C	CNTs/ wt%	MC/ wt%	TBP/ wt%	PS/ wt%
S25-B-0	0.25	0.00	0.00	0.15	0.60
S25-B-1	0.25	0.05	0.10	0.15	0.60
S25-B-2	0.25	0.10	0.15	0.15	0.60
S25-B-3	0.25	0.12	0.20	0.15	0.60
S25-B-4	0.25	0.15	0.24	0.15	0.60
S30-B-0	0.25	0.00	0.00	0.15	0.20
S30-B-1	0.25	0.05	0.10	0.15	0.20
S30-B-2	0.25	0.10	0.15	0.15	0.20
S30-B-3	0.25	0.12	0.20	0.15	0.20
S30-B-4	0.25	0.15	0.24	0.15	0.20
S35-B-0	0.25	0.00	0.00	0.15	0.00
S35-B-1	0.25	0.05	0.10	0.15	0.00
S35-B-2	0.25	0.10	0.15	0.15	0.00
S35-B-3	0.25	0.12	0.20	0.15	0.00
S35-B-4	0.25	0.15	0.24	0.15	0.00

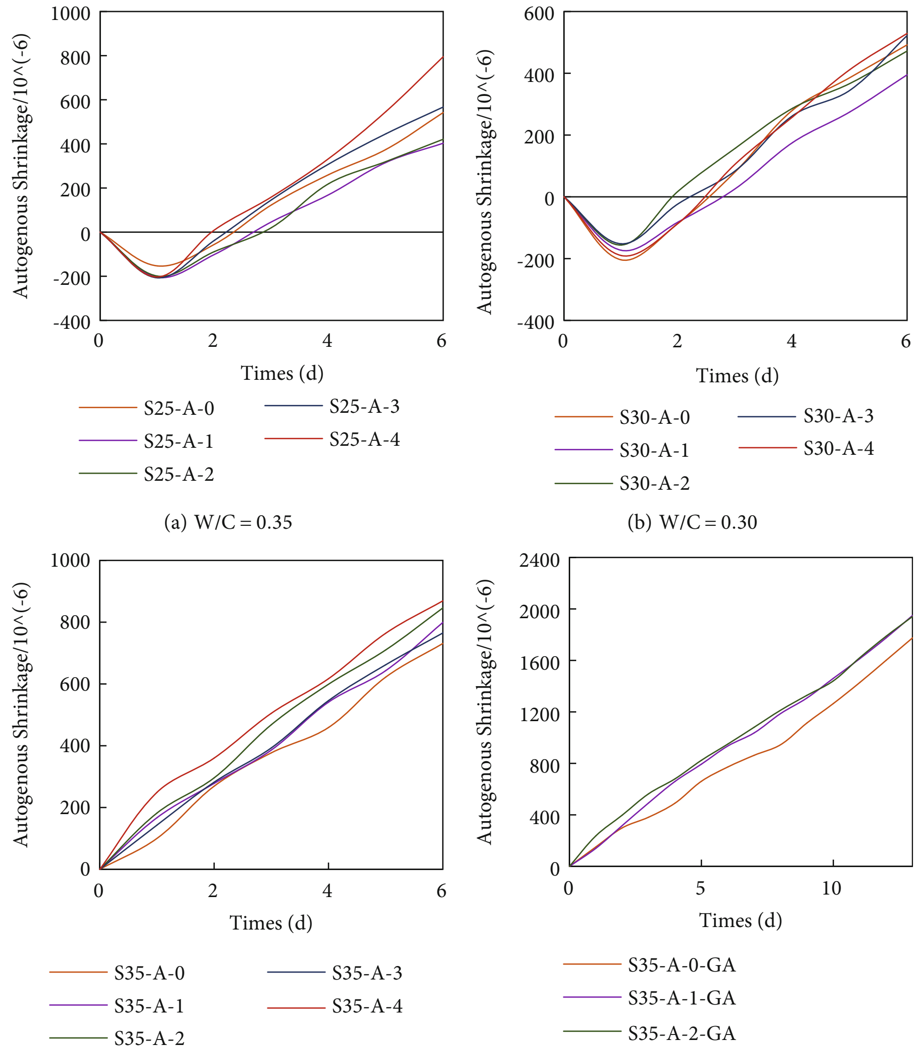

(a) W/C = 0.35 (b) W/C = 0.30

(c) W/C = 0.25 (d) W/C = 0.25 (influence of GA)

Figure 2: Self-shrinkage changes of new energy materials with different nano and lime ratios.

self-shrinkage value presents a positive value. However, when the water-cement ratio is 0.25, even on the first day of measurement, the self-shrinkage value of the specimen is much greater than the thermal expansion value, so the self-shrinkage value of the specimen increases with the increase of age.

(2) Under the same water-cement ratio, the self-shrinkage of multiwalled carbon nanotube cement paste changes with the change of carbon nanotube content.

It can be seen from these four figures that, under the condition of a certain water-cement ratio, with the increase of the content of multiwalled carbon nanotubes, the self-shrinkage value of multiwalled carbon nanotube cement paste first decreases and then increases. When the water-cement ratio is 0.35 and the test age is 7 days, the self-shrinkage value of cement paste containing 0.05 wt% MWCNTs is the smallest, which is 46.74% lower than that of the blank sample. In addition, when the water-cement ratio is 0.30 and the measurement age is 7 days, the optimum content of multiwalled carbon nanotube cement paste is 0.075 wt%, and the reduction rate of self-shrinkage value is 45.37% compared with the blank specimen under the same conditions. When the water-cement ratio is 0.25 and the measurement age is 7 days and 14 days, respectively, the optimum content of multiwalled carbon nanotube cement paste sample is 0.075 weight, and the self-shrinkage value is reduced by 9.32% and 11.54%, respectively, compared with the blank sample. It can also be observed from the figure that when the doping amount of multiwall carbon nanotubes reaches 0.12 wt%, the self-shrinkage value of the cement paste specimen containing multiwall carbon nanotubes is greater than that of the reference sample. It can be inferred that the high content of multiwalled carbon nanotubes limits the dispersion of multiwalled carbon nanotubes in the cement matrix, resulting in poor dispersion and aggregation of multiwalled carbon nanotubes in the cement matrix. This not only fails to give full play to the advantages of multiwalled carbon nanotubes, but also causes interface

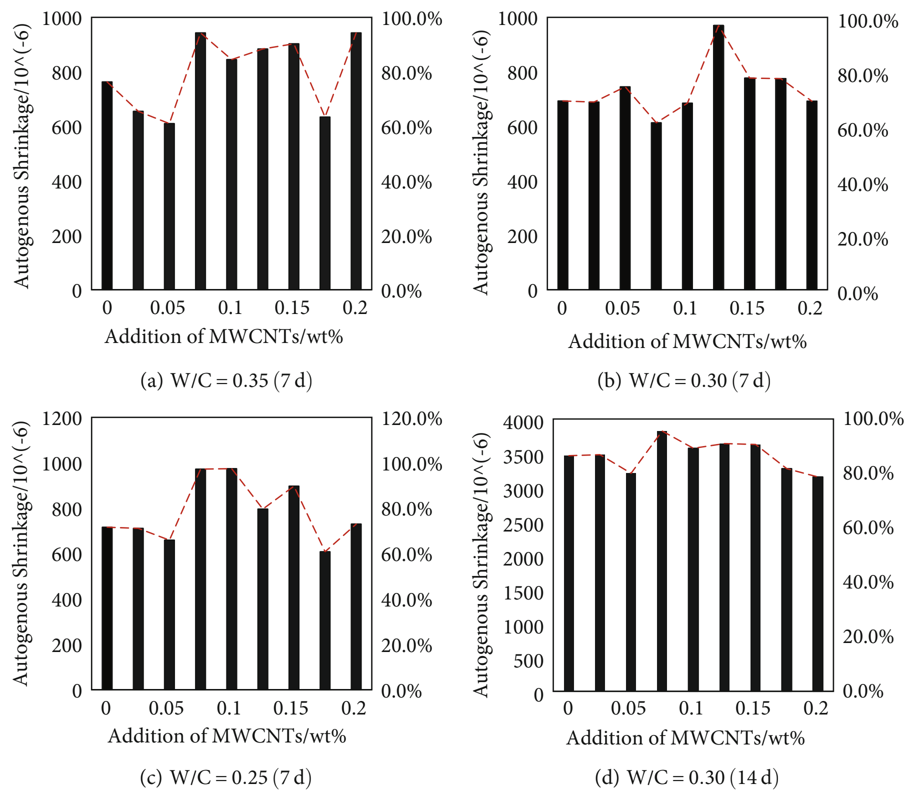

Figure 3: Variation of self-shrinkage value of nanomaterials under different water-cement ratio.

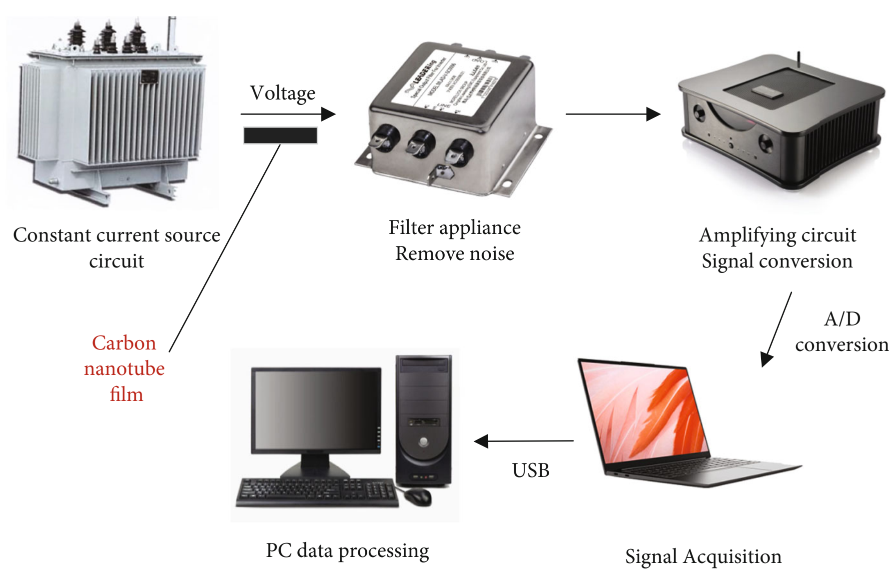

Figure 4: Hardware circuit design block diagram.

defects between multiwalled carbon nanotubes and cement matrix, which brings harm to cement-based materials and increases the self-shrinkage value of specimens [28]. Under a certain water-cement ratio, the auto-shrinkage performance of the multiwalled carbon nanotube cement slurry varies with its content, as shown in Figure 3.

The experimental results of self-shrinkage of carbon nanomaterials are as follows. When the ratio of water to cement is 0.3 and 0.35, the self-shrinkage value of carbon nanomaterial cement paste first decreases and then increases with the increase of age. When the ratio of water to cement is 0.25, the self-shrinkage value of the test piece increases with the increase of age, especially from the initial setting time to the second day of the test age. When the test age increases to 7 d (w/C = 0.35 and 0.30) or 14 d (w/C = 0.25), the growth rate of autogenous shrinkage value of carbon

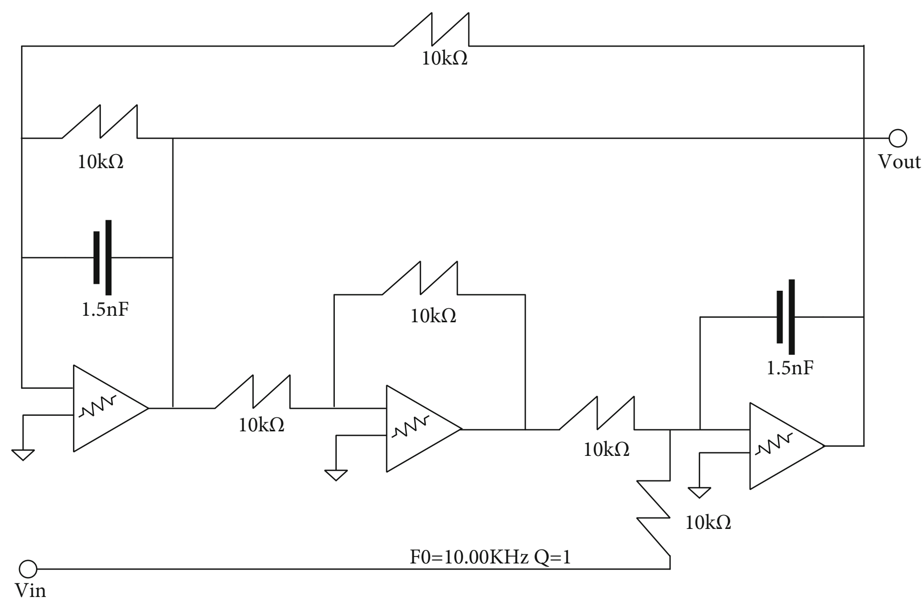

Figure 5: Simulation diagram of third-order Butterworth filter.

nanomaterial cement paste will decrease, but the growth rate of autogenous shrinkage value is slow. Under the same water-cement ratio, with the increase of carbon nanomaterial content, the self-shrinkage value of carbon nanomaterial cement paste first decreases and then increases [29]. When the water-cement ratio is 0.35 and the test age is 7 days, the self-shrinkage value of cement paste containing 0.05 wt% carbon nanomaterial is the smallest, which is 46.74% lower than that of the blank sample. When the content of carbon nanomaterial reaches 0.12 wt%, the self-shrinkage value of carbon nanomaterial cement paste sample is greater than that of the blank sample. The greater the content of carbon nanomaterial, the greater the self-shrinkage value of cement paste.

3.3. Application of Carbon Nanomaterials. This part mainly studies the hardware circuit design of polymer-based composite health monitoring data acquisition system based on carbon nanotube thin film sensor. The system is mainly composed of power supply circuit, constant current source circuit, filter circuit, amplification circuit, data acquisition circuit, and main computer. The communication circuit is composed of real-time online detection of basic parameters such as resistance value, film temperature, and film distortion state of the film sensor during composite deformation [30]. The block diagram of hardware design is shown in Figure 4.

Compared with other filters, the amplitude characteristic curve in the passband of Butterworth filter is almost parallel, there is no obvious fluctuation, and the useful signal can pass through almost without attenuation. For the clutter signal above this frequency, the amplitude curve shows a strict downward trend, the interference with the signal is stronger and stronger, and the filtering accuracy is higher and higher. However, the transition band is long, and the clutter signal processing effect near the cut-off frequency is not obvious. After filter simulation, the circuit design scheme and spectrum diagram of the curve are obtained, as shown in Figure 5 and Figure 6.

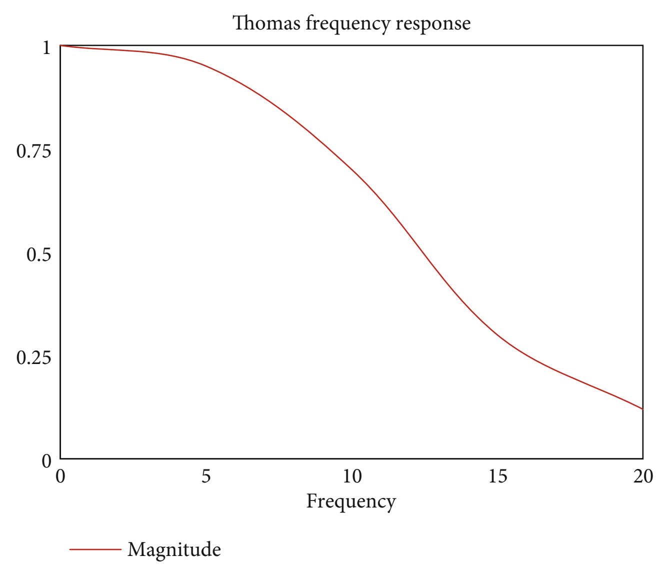

Figure 6: Amplitude frequency diagram of third-order Butterworth filter.

It can be seen from the amplitude-frequency diagram of Butterworth filter that the curve is strictly monotonically decreasing. When the amplitude is -3 dB, the passband gain is 0.7, and the corresponding cut-off frequency is 9.982 khz, which is a little different from the ideal value of 10 kHz. However, the transition band is relatively flat, and the filter gain corresponding to 12.5 k frequency is as high as 0.5, which has no obvious effect on the clutter near the cut-off frequency.

Generally, the damage mode of large structural members has the following two characteristics: the uncertainty of damage location and the randomness of damage direction, which poses a great challenge to the current real-time

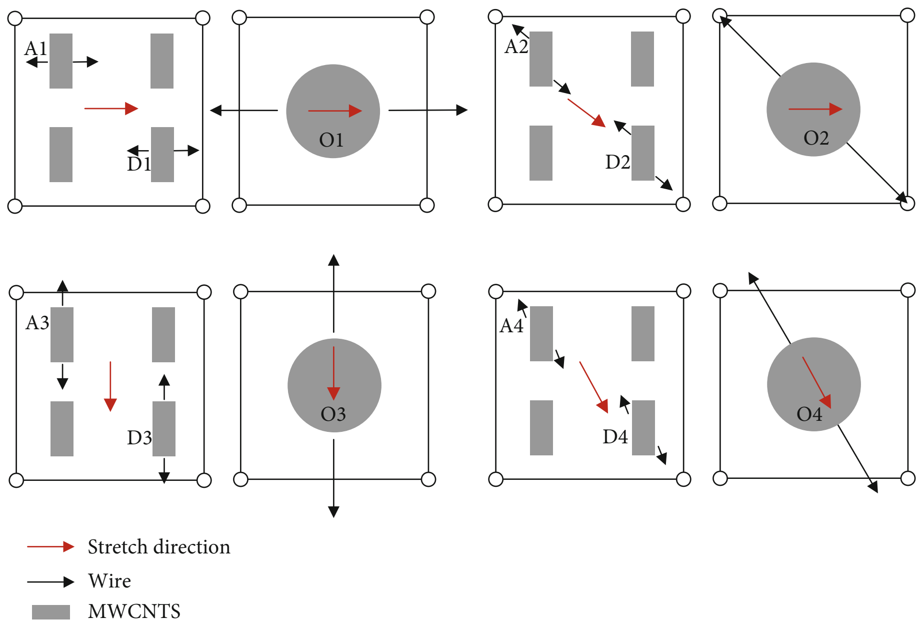

Figure 7: Multiangle tensile comparison test of rectangular sensor and omnidirectional sensor.

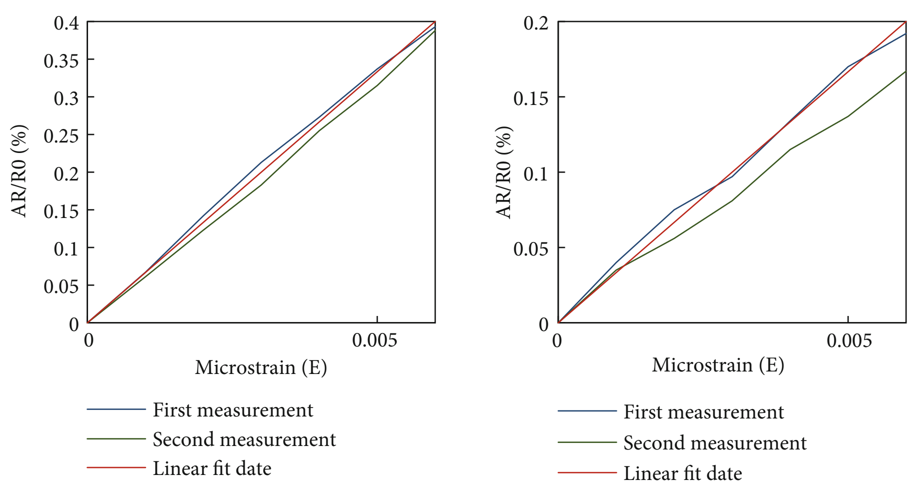

Figure 8: Tensile test results of rectangular sensor at 0° and 90°.

condition monitoring method of large structural members. In view of this situation, this paper puts forward the following design scheme. Traditional rectangular sensors are distributed in matrix composites in an array manner to detect different areas of the structure online and in real time. The scheme is shown in Figure 7.

For the first scheme, when the composite substrate is locally bent and deformed, four rectangular sensors with different orientations will produce different strain characteristics, resulting in some differences in the fluctuation value of the resistance change rate. By comparing the data fluctuation, the position of bending deformation can be preliminarily determined. However, because the sensor pasting method of the traditional rectangular sensor is synchronized with the fiber direction of the tested polymer matrix composite, the rectangular sensor can collect the change value of resistivity in the fiber direction in real time. However, when the fission direction of the composite substrate is in the vertical direction or any angle of the optical fiber, there is a certain measurement error in the distribution mode of the rectangular sensor array. The measured resistance value is only the vertical component of the optical fiber direction, which cannot well reflect the strain state of the material. Therefore, in the comparative test of this paper, this paper will further verify whether the rectangular sensor has omnidirectional characteristics and test whether the rectangular sensor has omnidirectional monitoring capability of composite materials.

The experimental results of data processing are shown in Figure 8. Because the four sensors are symmetrically distributed in the array, their deformation states are completely consistent. This paper takes the sensor in the upper left corner as a representative for real-time data analysis. It is found that there is always a strict linear relationship between the resistance change rate of the film sensor and the tensile stress whether the film detection direction is along the horizontal or vertical direction. In the range of 0-6000ue, with the increase of tensile stress, △ R/R0 increases linearly. Carbon nanotube films are very sensitive to small strains. During the loading process, the change rate of resistance is positively correlated with the increase of tensile strain. Through the linear fitting of the least square method, the tensile strain sensing equation of the rectangular thin film sensor is $\triangle R/R0 = 70e - 0.5$ along the optical fiber direction and $\triangle R/R0 = 40e - 0.1$ along the vertical direction of the optical fiber. The sensitivity coefficients of the two directions are quite different, and the feedback damage information of the same material in different directions is different, so there is a certain measurement error.

4. Discussion

With the diversification of application fields, materials are often affected by complex mechanical loads, multiphysical field coupling, and even corrosive environment. The research of carbon nanomaterials, carbon nanofibers, and graphene-based composites is still in the exploratory stage, and further research is needed in many aspects. This paper needs to further study the total shrinkage of carbon nanomaterial and cement-based composites. The shrinkage of cement materials also includes drying shrinkage, plastic shrinkage, carbonization shrinkage caused by carbonization, chemical shrinkage, and cold shrinkage caused by temperature reduction. The conditions can further test the total shrinkage value of carbon nanomaterials and cement-based composites and study the effects of carbon nanomaterials, carbon nanofibers, and graphene on the total shrinkage properties of cement-based materials.

5. Conclusions

With the increase of water-cement ratio, the self-shrinkage of cement paste specimen decreases clearly. When the water-cement ratio is 0.25, the self-shrinkage value of 0.05% carbon nanomaterial cement paste is 74.68% lower than that when the water-cement ratio is 0.30. In the experimental study of omnidirectional monitoring characteristics, through the repeated tensile tests of rectangular sensor and omnidirectional sensor at 0°C, 30°C, 60°C, and 90°C, it is found that the sensitivity coefficient of rectangular sensor is quite different from the short side, but the sensitivity coefficient of omnidirectional sensor fluctuates slightly in different directions, ranging from 55.8 to 60.4, and the maximum fluctuation is only 5. This fully proves that the carbon nanotube omnidirectional sensor has omnidirectional detection ability.

Data Availability

The data underlying the results presented in the study are available within the manuscript.

Conflicts of Interest

The authors declare that they have no conflicts of interest.

References

[1] Q. Wang, "Teaching reform of organic chemistry in new energy materials and devices specialty under the background of establishing the emerging engineering education," *University Chemistry*, vol. 34, no. 7, pp. 42–46, 2019.

[2] F. Martinho, A. Hajijafarassar, S. L. Marino et al., "Nitride-based interfacial layers for monolithic tandem integration of new solar energy materials on Si: the case of CZTS," *ACS Applied Energy Materials*, vol. 3, no. 5, pp. 4600–4609, 2020.

[3] Z. A. Mansurov, M. K. Atamanov, Z. Elemesova, B. T. Lesbaev, and M. N. Chikradze, "New nanocarbon high-energy materials," *Combustion Explosion and Shock Waves*, vol. 55, no. 4, pp. 402–408, 2019.

[4] J. Paben, "How a materials recovery facility will sort flexible plastics," *Resource Recycling*, vol. 38, no. 1, pp. 11–11, 2019.

[5] K. W. Tao, A. L. Zhang, A. J. Cai et al., "Simulation studies of the granular flow beryllium target for the compact materials irradiation facility," *Nuclear Instruments and Methods in Physics Research*, vol. 942, pp. 162401.1–162401.6, 2019.

[6] J. Y. Lee, Y. C. Choi, and J. W. Lee, "The effect of participation motivation in the university sports facility users on Servicescape: differences in students and local residents," *Korean Journal of Sports Science*, vol. 29, no. 5, pp. 463–474, 2020.

[7] I. Setiawan and T. Anggah, "Customer satisfaction with fitness services and equipment facilities in gym academic faculty of science of science, Jakarta State University[j]," *Gladi Jurnal ILMU Keolahragaan*, vol. 12, no. 1, pp. 42–47, 2021.

[8] T. S. Thakur and P. M. Babu, "Evolution of bicycles and their utility as fitness aids -a review," *Nursing and Health Sciences*, vol. 8, no. 3, pp. 19–23, 2019.

[9] L. Zhou, F. Li, L. Wang, Y. Wang, and G. Wang, "A new energy consumption model suitable for processing multiple materials in end milling," *The International Journal of Advanced Manufacturing Technology*, vol. 115, no. 7-8, pp. 2521–2531, 2021.

[10] E. K. Jang, J. Im, J. Ahn, S. Yoon, and K. Y. Cho, "Layer design and approach in new energy storage materials," *ECS Meeting Abstracts*, vol. 2, 2020.

[11] B. Gao, X. Ning, and P. Xing, "Shock wave induced nanocrystallization during the high current pulsed electron beam process and its effect on mechanical properties," *Materials Letters*, vol. 237, no. 15, pp. 180–184, 2019.

[12] P. Wang, S. Wang, X. Zhang et al., "Rational construction of CoO/CoF2 coating on burnt-pot inspired 2D CNs as the battery-like electrode for supercapacitors," *Journal of Alloys and Compounds*, vol. 819, p. 153374, 2019.

[13] C. M. Lampert, G. Smestad, K. L. Chopra, A. Roos, and H. Takakura, "Smestad and solar energy materials and solar Cells," *Solar Energy Materials and Solar Cells*, vol. 194, pp. A1–A3, 2019.

[14] N. Navarro, R. Kajiura, A. Miura, and K. Tadanaga, "Organic–inorganic hybrid materials for interface design in all-solid-state batteries with a Garnet-type solid electrolyte," *ACS Applied Energy Materials*, vol. 3, no. 11, pp. 11260–11268, 2020.

[15] Y. Tang, Z. Chen, W. Feng, Y. Nong, C. Li, and J. Chen, "Combined effects of nano-silica and silica fume on the mechanical behavior of recycled aggregate concrete," *Nanotechnology Reviews*, vol. 10, no. 1, pp. 819–838, 2021.

[16] C. Giannoulakis, "Sport facility & event management," *International Journal of Sport Communication*, vol. 12, no. 4, pp. 606–609, 2019.

[17] W. Suk and J. Y. Han, "impact of a new sport facility for urban regeneration: a case of DGB Daegu Bank Park," *Korean Journal of Sport Management*, vol. 26, no. 3, pp. 52–69, 2021.

[18] T. Kim and S. K. Min, "A comparative advantage analysis of regional leisure sport facility industry," *Korean Journal of Sport Management*, vol. 25, no. 4, pp. 113–124, 2020.

[19] G. Oseghale, "Sports facilities condition assessment in selected universities in south western Nigeria," *IOSR Journal of Sports and Physical Education*, vol. 8, no. 2, pp. 1–07, 2021.

[20] P. R. Milton, L. M. Williamson, K. Brubaker, and M. Papania, "Recreate and retain: how entrance into a campus recreation facility impacts retention," *Recreational Sports Journal*, vol. 44, no. 2, pp. 89–98, 2020.

[21] L. Capasso, D. D'Alessandro, V. I. Popov, I. I. Libina, and I. I. Torubarova, "Hygienic requirements for the construction and operation of sports facilities in the Russian Federation and Italy," *Review Manuscrip. Gigiena i Sanitariia*, vol. 99, no. 1, pp. 20–25, 2020.

[22] G. Grossman, V. Beck, W. Dan, E. Toklu, and M. El-Sayed, "Application of a continuously active antimicrobial surface coating in two professional sports training facilities," *Infection Control and Hospital Epidemiology*, vol. 41, no. 1, pp. s440–s440, 2020.

[23] A. A. Kim, Y. Sunitiyoso, and L. A. Medal, "Understanding facility management decision making for energy efficiency efforts for buildings at a higher education institution," *Energy and Buildings*, vol. 199, pp. 197–215, 2019.

[24] M. Parrott, J. Ruyak, and G. Liguori, "The history of exercise equipment: from sticks and stones to apps and phones," *ACSM s Health & Fitness Journal*, vol. 24, no. 6, pp. 5–8, 2020.

[25] A. Freitas and T. S. Lacerda, "Fitness centers: what are the most important attributes in this sector?," *International Journal for Quality Research*, vol. 13, no. 1, pp. 177–192, 2019.

[26] Z. Arifin, S. D. Prasetyo, S. Suyitno et al., "Rancang Bangun Alat elliptical trainer outdoor," *Mekanika Majalah Ilmiah Mekanika*, vol. 19, no. 2, pp. 104–112, 2020.

[27] B. Gopi, M. Di Canio, N. Chintalapudi, F. Amenta, and G. Nittari, "Development of physical training smartphone application to maintain fitness levels in seafarers," *International Maritime Health*, vol. 70, no. 3, pp. 180–186, 2019.

[28] X. Zhao, Y. Dong, X. Yuan, J. Li, Y. Zhao, and Z. Bao, "Improvement of unmanned aerial vehicle cluster atmospheric monitoring algorithms," *Journal of Environmental Protection and Ecology*, vol. 20, no. 3, pp. 1068–1075, 2019.

[29] J. Eickhoff-Shemek, "HIIT for clinical populations: safety and legal liability issues for community fitness facilities," *ACSM s Health & Fitness Journal*, vol. 25, no. 5, pp. 65–67, 2021.

[30] F. Qian, "State council: strengthen the construction of public fitness venues and facilities to develop mass sports," *China City Planning Review*, vol. 29, no. 4, pp. 6–6, 2020.